Environmental Modelling & Software 24 (2009) 1163–1170

Contents lists available at ScienceDirect

Environmental Modelling & Software

journal homepage: www.elsevier.com/locate/envsoft

Comparison of interpolation methods for depth to groundwater and its temporal and spatial variations in the Minqin oasis of northwest China

Yue Sun [a], Shaozhong Kang [a,*], Fusheng Li [b], Lu Zhang [c]

[a] Center for Agricultural Water Research in China, China Agricultural University, East Campus, Beijing 100083, China
[b] Agricultural College, Guangxi University, Nanning, Guangxi 530005, China
[c] CSIRO Land and Water, Christian Laboratory, GPO Box 1666, Canberra, ACT 2601, Australia

ARTICLE INFO

Article history:
Received 21 March 2009
Received in revised form
26 March 2009
Accepted 26 March 2009
Available online 6 May 2009

Keywords:
Autoregressive model
Geographic information system
Depth to groundwater
Minqin oasis
Interpolation method
Temporal and spatial variation

ABSTRACT

Severe water shortages and dramatic declines in groundwater levels have resulted in environmental deterioration in the Minqin oasis, an arid region of northwest China. Understanding temporal and spatial variations in the depth to groundwater in the region is important for developing management strategies. Depth to groundwater records for 48 observation wells in the Minqin oasis were available for 22 years from 1981 to 2003, allowing us to compare three different interpolation methods based on three selected years (1981, 1990, 2002) as starting points. The three methods were inverse distance weighting (IDW), radial basis function (RBF), and kriging (including ordinary kriging (OK), simple kriging (SK), and universal kriging (UK)). Cross-validation was applied to evaluate the accuracy of the various methods, and two indices – the correlation coefficient (R^2) and the root mean squared error (*RMSE*) – were used to compare the interpolation methods. Another two indices – deviation of estimation errors (σ) and 95% prediction interval (95 PPI) – were used to assess prediction errors. Comparison of interpolated values with observed values indicates that simple kriging is the optimal method for interpolating depth to groundwater in this region: it had the lowest standard deviation of estimation errors and smallest 95% prediction interval (95 PPI). By using the simple kriging method and an autoregressive model for depth to groundwater based on the data from 1981 to 2003, this work revealed systematic temporal and spatial variations in the depth to groundwater in the Minqin oasis. The water table has declined rapidly over the past 22 years, with the average depth to groundwater increasing from 4.95 m in 1981 to 14.07 m in 2002. We attribute the decline in the water table to excessive extraction and to decreases in irrigation channel leakage.

1. Introduction

Minqin oasis, in the arid inland of northwest China, is a region with a fragile ecosystem and a severe shortage of water resources. The oasis is located between the Tenggeli and Badanjilin deserts in the lower reaches of the Shiyang river, and has low rainfall and high potential evaporation. Inflow into Hongyashan reservoir has reduced every year over the past 30 years due to high water use in the upper part of the Shiyang river basin, which in turn has led to lower groundwater recharge. If continued, lack of water will result in water stress of plants in the area, and may finally result in desertification and severe environmental damage.

Understanding temporal and spatial variations of depth to groundwater is a prerequisite to achieving sustainable water use in the basin. Point measurements of watertable levels are available, but what is needed are groundwater surfaces based on these measurements. A robust interpolation method is needed to do this, and many have been discussed in the literature. Li et al. (2005) discussed a geometrical method, a statistical method, a variation using spatial statistics, a functional method, a technique using stochastic modeling, another using physical modeling, and finally an integrated method. Caruso and Quarta (1998) compared several interpolation methods and discussed advantages and disadvantages of each. Theodossiou and Latinopoulos (2006, 2007) interpolated the groundwater level in the Anthemountas basin of northern Greece using a kriging method and they estimated the accuracy of interpolated values using cross-validation. Among numerous interpolation methods, no method is uniquely optimal, and so the best interpolation method for a specific situation can only be obtained by comparing their results. Some research has been done on comparing different interpolation methods in a variety of situations, and use of geographic information systems

* Corresponding author. Fax: +86 10 62737611.
E-mail address: kangshaozhong@tom.com (S. Kang).

1364-8152/$ – see front matter © 2009 Elsevier Ltd. All rights reserved.
doi:10.1016/j.envsoft.2009.03.009

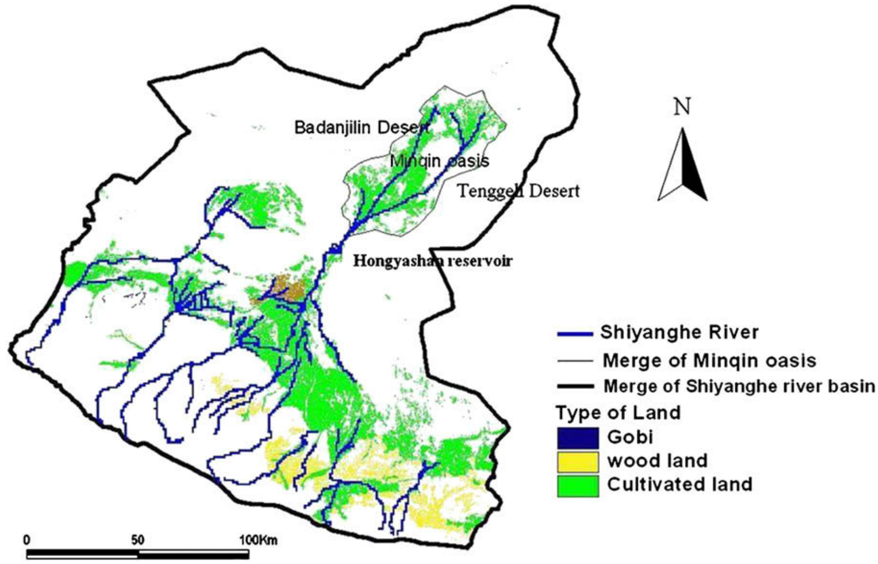

Fig. 1. Location of Minqin oasis in the Shiyang river basin.

(GIS) has been an important tool in analyzing the character of groundwater in particular areas (Hutchinson, 1995; Collins, 1996; Feng et al., 2004; Fang et al., 2005; Li et al., 2006; Kenneth, 1996; Wang et al., 2004; Wei et al., 2003; Xu and Cai, 2005). Nevertheless, there have been few reports comparing different interpolation methods for depth to groundwater in arid regions.

The objectives of this study were therefore firstly to select an optimal interpolation method in this region from among kriging methods (including ordinary kriging (OK), simple kriging (SK), and universal kriging (UK)), the inverse distance weighting (IDW) method, and the radial basis function (RBF) method. We did so by comparing the interpolation accuracy of depth to groundwater for each method and analyzing the errors. Secondly, we used the best interpolation method to analyze temporal and spatial variations of depth to groundwater. Finally, we analyzed the trend in depth to groundwater over the past 22 years using the Kendall method and developed an autoregressive prediction equation for depth to groundwater. Our results confirm that excessive groundwater extraction is causing severe groundwater declines in the Minqin oasis.

2. Materials and methods

2.1. Experimental site

Fig. 1 shows the general location of the Minqin oasis. The oasis itself (Fig. 2) occupies an area of 2868 km^2 (E 102°54′–103°49′, N 38°27′–39°07′, altitude 1309–1459 m). It is surrounded by hills and deserts, and slopes downwards from south-west to northeast. The climate is characterized by low rainfall (about 110 mm), high potential evaporation (2650 mm), intense sunshine, and strong wind. Cultivated land occupies 6.78×10^4 hm^2 and the main soil type is silty clay. Principal crops include cereals (spring wheat, summer maize) and cash crops (cotton, seed melon, and fennel) (Fang et al., 2005). Native vegetation is mainly drought-resistant shrub, salt-resistant shrub, and perennial sand-loving herbaceous plants (e.g. *Elaeagnus angustifolia*, *Populus euphratica*, and *Salix purpurea*) (Kang et al., 2004).

2.2. Data collection

The data used in this study were placed in a digital elevation model (DEM) of the Shiyang river basin with a grid resolution 100 × 100 m, and included longitude and latitude for each of 48 groundwater observation wells and the monthly average observed depth to groundwater over the period 1981–2003. The location of the 48 observation wells is shown in Fig. 3. Based on the monthly average depth, a dataset of average annual depth was established for each observation well and its geodetic coordinates. The dataset appeared as a spot layer in the geographic information system (GIS) (ESRI, 2004). Within the 22-year dataset, depth to groundwater in 1981, 1990, and 2002 was selected as reference points for comparing various interpolation methods.

2.3. Interpolation methods for depth to groundwater

To select the optimal method in this study, several interpolation methods – the inverse distance weighting (IDW) method, the radial basis function (RBF) method, and the kriging method – were compared, and then the optimal interpolation method was used to give the spatial distribution of depth to groundwater in different years.

2.3.1. Inverse distance weighting method

In the inverse distance weighting (IDW) method, the weightings are solely a function of the distance between the point of interest and the sampling points for $i = 1, 2, \ldots, n$. Considering the distance D_i between these two points, the value of a point of interest point takes the form:

$$Z = \frac{\sum_{i=1}^{n} \frac{1}{(D_i)^q} Z_i}{\sum_{i=1}^{n} \frac{1}{(D_i)^q}}, \quad (1)$$

where Z is the interpolated value of the point of interest; Z_i is the value of sampling point i ($i = 1, \ldots, n$); D_i is the distance between the interpolated and sampled values; and q is an appropriate constant. If the parameter q takes a value of 1 or 2, the method is called, respectively, inverse distance interpolation or inverse distance squared interpolation (Ashraf et al., 1997). In this study q was set to 2.

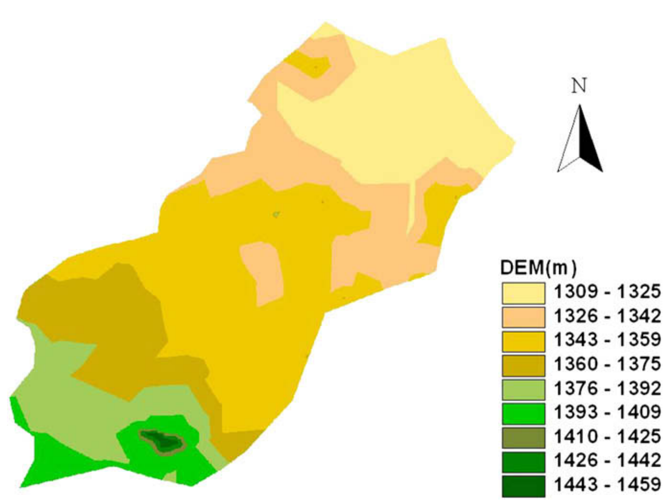

Fig. 2. Digital elevation model (DEM) for Minqin oasis.

2.3.2. Radial basis function (RBF) method

The radial basis function (RBF) method is one derived from neural networks (Chen et al., 1991). The RBF neural network has a feed-forward architecture, which consists of three layers: one input layer, one hidden layer, and one output layer, with a number of neurons in each. Such a network possesses self-organizing characteristics that allow for adaptive determination of the hidden neurons during training of the network (Zhang and Kushwaha, 1999). Each input neuron is completely connected to all hidden neurons, and hidden neurons and output neurons are also interconnected to each other by a set of weights. Information fed into the network through input neurons is transmitted to the hidden neurons; each hidden neuron then transforms the input signal using a transfer function f. The output of hidden neurons has the form of a radial basis function.

For the present model, a Gaussian function was selected for the RBF. The Gaussian is a positive radial symmetric function (kernel) with center μ and spread σ. The spread – called the receptive field ($\mu \pm \sigma$) of a hidden neuron – is the radial distance from the center of kernel within which the value of the function differs significantly from zero. An input pattern falling within the receptive field will cause a significant response. For each input pattern, the hidden neurons compute the distance between the input signal and the center of the receptive field. For a Gaussian function, the response is unity if this distance is zero, and decays to zero when the distance is greater than the spread. The response of the jth hidden neuron h_j to an input signal X is given by

$$h_j = f\left[-\frac{\|X-\mu_j\|}{2\sigma_j^2}\right], \quad j = 1,2,\ldots,j \tag{2}$$

where $\|\bullet\|$ is the Euclidean distance and μ_j and σ_j are respectively the center and spread of hidden neuron j. The responses are multiplied by the interconnect weights W between the hidden and output layers. Each unit in the output layer then makes a linear transformation on the data from the hidden layer. For instance, the response y_k of neuron k can be expressed as:

$$y_k = \sum_{j=1}^{J} h_j W_{kj}, \quad k = 1,2,\ldots,k \tag{3}$$

where W_{kj} is the connection weight between the hidden neuron j and output neuron k. To train our RBF network, the orthogonal least squares (OLS) algorithm proposed by Chen et al. (1991) was used to self-organize the hidden neurons. Beginning with zero neurons, the hidden neurons are added one by one until the output of the trained network is within a targeted precision. The sum of the squared error from the network is computed for each iteration. If the error is lower than a predefined tolerance (sum of squared error), the training is stopped and the number of neurons added to the hidden layer represents the number of hidden neurons required. If the sum of the squared error is above the tolerance then the input pattern with the largest error is identified and added to the hidden layer, which results in maximum lowering of the network error. This process is repeated until the error value falls below the tolerance value (Demuth and Beale, 1996).

2.3.3. Kriging method

The kriging method, which is referred to as partial spatial estimation or interpolation, is the best linear unbiased method to estimate the value of regionalized variables at an unsampled location based on the available data of regionalized variables and structural features of a variogram. It can be classified into simple kriging (SK), ordinary kriging (OK), and universal kriging (UK).

If n is the number of values used for the estimation and m is the mean, then the estimator of simple kriging is:

$$Z^*(x_0) = m + \sum_{i=1}^{n} \lambda_i [Z(x_i) - m] \tag{4}$$

where $Z^*(x_0)$ is the estimate value at x_0, $Z(x_i)$ is the measure value at the x_i; λ_i is the weight assigned for the residual of $Z(x_i)$, and their summation is 1 (Li et al., 2000; Zhang, 2005).

The estimator of ordinary kriging is given by

$$Z^*(x_0) = \sum_{i=1}^{n} \lambda_i Z(x_i) \tag{5}$$

where the variables are defined as before.

Considering the deterministic (drift) component, universal kriging is a geostatistics method for linear unbiased estimator in which the column vector of the covariance for non-statistical random function and variogram is given. By definition of the drift component, the expected value of $Z(x)$ at point Z is $m(x)$:

$$E[Z(x)] = m(x) \tag{6}$$

The interpolation expressions take the form of

$$Z^*(x_0) = \sum_{i=1}^{n} \lambda_a Z_a \tag{7}$$

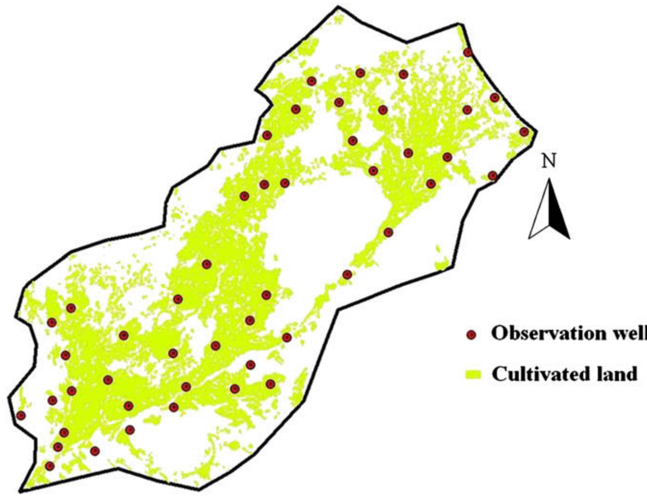

Fig. 3. Location of observation wells in the Minqin oasis.

where n is the number of available sampling data, $Z^*(x_0)$ is the estimated value, Z_a is the measured value at sampling point a ($a = 1, \ldots, n$), and λ_a is the weighting coefficient, which is calculated with the unbiased and minimum error variance.

2.4. Cross-validation

The cross-validation method is used to assess which method gives the best interpolation. In a cross-validation exercise, the estimation method is tested at the locations of existing samples. The sample value at a particular location is temporarily discarded from the sample dataset, and the value at the same location is then estimated using the remaining samples. Once the estimate is calculated, one can compare it to the true sample value that was initially removed from the sample dataset. This procedure is repeated for all available samples. The resulting true and estimated values can then be compared using statistics (Zhang, 2005). In this way, we calculated the error between the true value and the estimated value so as to gauge the precision of each interpolation method.

The main selected criterion of cross-validation is root mean squared error (*RMSE*), which can take into account stationary points and extrema, and can be calculated as follows:

$$RMSE = \sqrt{\frac{1}{n}\sum_{i=1}^{n}(Z_i - Z)^2} \tag{8}$$

where Z is the estimated value; Z_i is the measured value at sampling point i ($i = 1, \ldots, n$); m is the number of selected parameters in the empirical equation; and n is the number of values used for the estimation.

Another criterion to assess the interpolation method is the correlation coefficient (R^2), which can summarize the correlation between the observed and estimated values.

2.5. Analysis of uncertainties in prediction

In the interpolated prediction, factors such as the number of nearby samples, the proximity of the available samples, the spatial arrangement of the samples (clustering), and the nature of the phenomenon under study will influence the results.

Table 1
Comparison of correlation coefficient between observed value of depth to groundwater and simulated value by three methods and *RMSE* of the simulated value by various methods.

Method	1981		1990		2002	
	RMSE (m)	R^2	*RMSE* (m)	R^2	*RMSE* (m)	R^2
IDW	1.63	0.41	2.63	0.58	3.98	0.68
SK	**1.47**	**0.56**	**2.08**	**0.73**	**3.87**	**0.70**
OK	1.86	0.39	2.35	0.61	4.23	0.65
UK	1.96	0.37	2.53	0.59	4.26	0.64
RBF	1.71	0.40	2.24	0.68	4.10	0.67

R is the correlation coefficient; *RMSE* is root mean square error. The symbols IDW, SK, OK, UK and RBF stand for methods explained in the text.

Table 2
Statistical results of depth to groundwater for 48 observation wells.

Year	Mean depth (m)	Minimum depth (m)	Median depth (m)	Maximum depth (m)	Decline rate (m a^{-1})	Mean decline rate (m a^{-1})
1981	4.95	0.76	4.84	11		
1990	8.43	1.08	9.84	17	0.38	0.43
2002	14.07	1.85	12.16	27.55	0.47	
Changing trend	↓	↓	↓	↓	↓	

The standard deviation of the estimation error (σ) is an index of uncertainty based on the number of nearby data points, the proximity of the samples, and also the interaction between the various factors, and is defined as:

$$\sigma = \sqrt{\sigma^2 + \sum_{i=1}^{n}\sum_{j=1}^{n}\lambda_i\lambda_j C_{ij} - 2\sum_{i=1}^{n}\lambda_i C_{oi}} \tag{9}$$

where σ^2 represents the variance of point values. The second term within the square root is a weighted sum of all the covariance between the various sample pairs and measures the degree of clustering. The third term is a weighted sum of the covariance between the samples and the value being estimated and it measures the proximity to each other of the available samples. The estimate is most reliable when it operates on an extremely smooth and well-behaved variable and the samples are not too close together but close to the samples being estimated.

2.6. Autoregressive model

The autoregressive model is a simple method for depth to groundwater prediction. The model does not take other factors into account and depends solely on depth to groundwater in past years to establish the equation:

$$H_t = \sum_{i=1}^{m}\varphi_i H_{t-i} + \varepsilon \tag{10}$$

where φ_i and ε are the autoregressive parameters; H_t is the depth to groundwater at year t; H_{t-i} is the depth to groundwater at year $t-i$; and m is the autoregressive rank, which can often be obtained with the least variance.

2.7. Kendall's rank correlation test

Kendall's rank correlation (or τ test), which is based on the proportionate number of subsequent observations that exceed a particular value, has been commonly used to assess the significance of trends in hydro-meteorological time series (Kendall and Stuart, 1973; Kottegoda, 1980). For a sequence $x_1, x_2, \ldots, x_n$, the standard procedure is to determine the number of times, say p, in all pairs of observations ($x_i, x_j; j > i$) that x_j is greater than x_i; the ordered (i, j) subsets are ($i = 1$, $j = 2, 3, \ldots, n$), ($i = 2, j = 3, 4, \ldots, n$), …, ($i = n-1, j = n$), where n is the dataset record length. This is a rising trend where succeeding values are always greater than preceding ones and p is given by $(n-1) + (n-2) + \ldots + 1$, which is the sum of an arithmetic progression and is given by $n(n-1)/2$. If the observations are totally reversed, $p = 0$ and it follows that, for a trend-free series,

$$E(p) = \frac{n(n-1)}{4} \tag{11}$$

The test is based on the statistic τ,

$$\tau = \frac{4p}{n(n-1)} - 1 \tag{12}$$

For a random sequence,

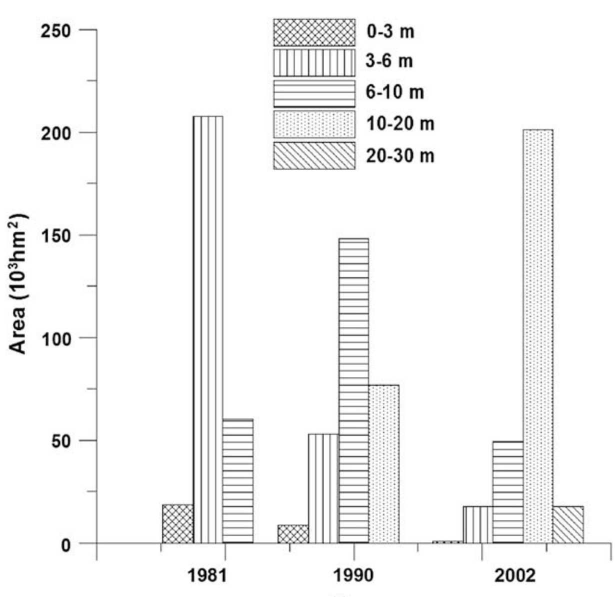

Fig. 4. Distribution of depths to groundwater in the Minqin oasis for 1981, 1990, and 2002.

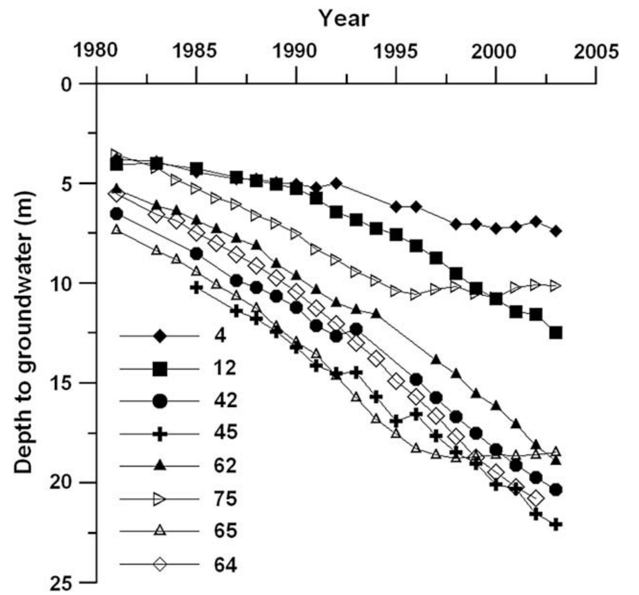

Fig. 5. Increase in depth to groundwater over the past 22 years for eight selected observation wells in the Minqin oasis.

Table 3
Average depth to groundwater over each period in the past 22 years for eight selected observation wells in the Minqin oasis.

Period	Well number							
	4#	12#	42#	45#	62#	64#	65#	75#
1981–1989	4.53	4.60	9.51	11.81	7.41	8.03	10.13	5.65
1990–1999	6.29	8.13	15.03	16.75	13.05	15.33	17.13	9.92
2000–2003	7.17	11.82	19.73	21.32	18.04	20.50	18.58	10.17
Changing trend	↓**	↓**	↓**	↓**	↓**	↓**	↓**	↓**

Note: ↓ indicates a decreasing trend, *significant level = 0.05, and ** significant level = 0.01.

Table 4
Parameters of an autoregressive model for depth to groundwater of eight selected observation wells and correlation coefficient between simulated value and measured value in the Minqin oasis.

Well number	Location	Parameters						R^2
		a	b	c	d	e	f	
4	Dongzhen	0.66	0.65	0.73	−0.75	−0.23	0.56	0.90
12	Zhongqu	0.13	0.92	0.24	−0.95	0.70	0.20	0.99
42	Hongshaliang	1.23	0.64	0.14	0.15	−0.01	0.10	0.97
45	Hongluyuan	2.22	−0.13	−0.18	0.54	0.40	0.43	0.99
62	Qinfeng	0.45	0.53	0.15	0.03	0.12	0.30	0.99
64	Sanlei	0.18	1.30	0.42	−0.35	−0.31	−0.11	0.99
65	Xinhe	0.78	1.63	−0.61	0.12	−0.38	0.20	0.99
75	Jiahe	0.69	1.35	−0.63	0.42	0.02	−0.24	0.98

Table 5
Parameters of uncertainty analysis.

Method	1981		1990		2002	
	σ (m)	95 PPI (m)	σ (m)	95 PPI (m)	σ (m)	95 PPI (m)
IDW	0.22	($Z^*\pm0.44$)	0.42	($Z^*\pm0.84$)	0.72	($Z^*\pm1.44$)
SK	**0.17**	($Z^*\pm0.34$)	**0.33**	($Z^*\pm$**0.66**)	**0.70**	($Z^*\pm$**1.40**)
OK	0.23	($Z^*\pm0.46$)	0.37	($Z^*\pm0.74$)	0.77	($Z^*\pm1.54$)
UK	0.26	($Z^*\pm0.52$)	0.39	($Z^*\pm0.78$)	0.78	($Z^*\pm1.56$)
RBF	0.23	($Z^*\pm0.46$)	0.36	($Z^*\pm0.72$)	0.73	($Z^*\pm1.46$)

Note: Z^* is the estimated value.

$$E(\tau) = 0 \tag{13}$$

$$\mathrm{Var}(\tau) = \frac{2(2n+5)}{9n(n-1)} \tag{14}$$

The test defines the standard normal variate N as:

$$N = \frac{\tau}{[\mathrm{Var}(\tau)]^{0.5}} \tag{15}$$

N converges rapidly to a standard normal distribution as n increases. At a specified level of significance of α, a standard N_α value can be obtained from a table of standard normal distributions. If $|N| > N_{\alpha/2}$, a positive N indicates an increasing trend in the time series, and a negative N indicates a decreasing trend.

3. Results and discussion

3.1. Comparison of interpolation methods and analysis of uncertainties in prediction

Depth to groundwater in Minqin oasis was interpolated in turn using kriging methods (OK, SK, and UK), the inverse distance weighing (IDW) method, and the radial basis function (RBF) method for three selected years (1981, 1990, 2002). For each method we then compared the interpolated values with observed values. As shown in Table 1, the correlation coefficient (R^2) between the estimated and observed depth to groundwater and root mean squared error (*RMSE*) varied from 0.37 to 0.56 in 1981, 0.58 to 0.73 in 1990, and 0.64 to 0.70 in 2002; the corresponding RMSE for the three years was 1.47–1.96 m, 2.08–2.63 m, and 3.87–4.26 m. The correlation coefficient for the different methods was in the order SK > IDW > RBF > OK > UK, while the order of *RMSE* was the reverse for the selected three years, indicating that the maximal correlation coefficient and minimal *RMSE* are obtained by SK, the optimal method for interpolating depth to groundwater in this region.

One-sample Kolomogorov–Semirnov test showed that the series of depth to groundwater in 1981, 1990, and 2002 followed a normal distribution. In this study, Eq. (9) was used to analyze the uncertainties of the interpolation and 95% prediction intervals were calculated. As shown in Table 5, the standard deviation of estimation error for several interpolation methods ranged from 0.17 to 0.78, and the simple kriging method had the lowest standard deviation of estimation error and confidence interval, indicating that this method had the least uncertainties and the highest confidence intervals.

3.2. Temporal variation of depth to groundwater in Minqin oasis

The temporal and spatial variations of depth to groundwater in Minqin oasis were interpolated using the selected simple kriging method; afterwards the spatial and temporal distributions of

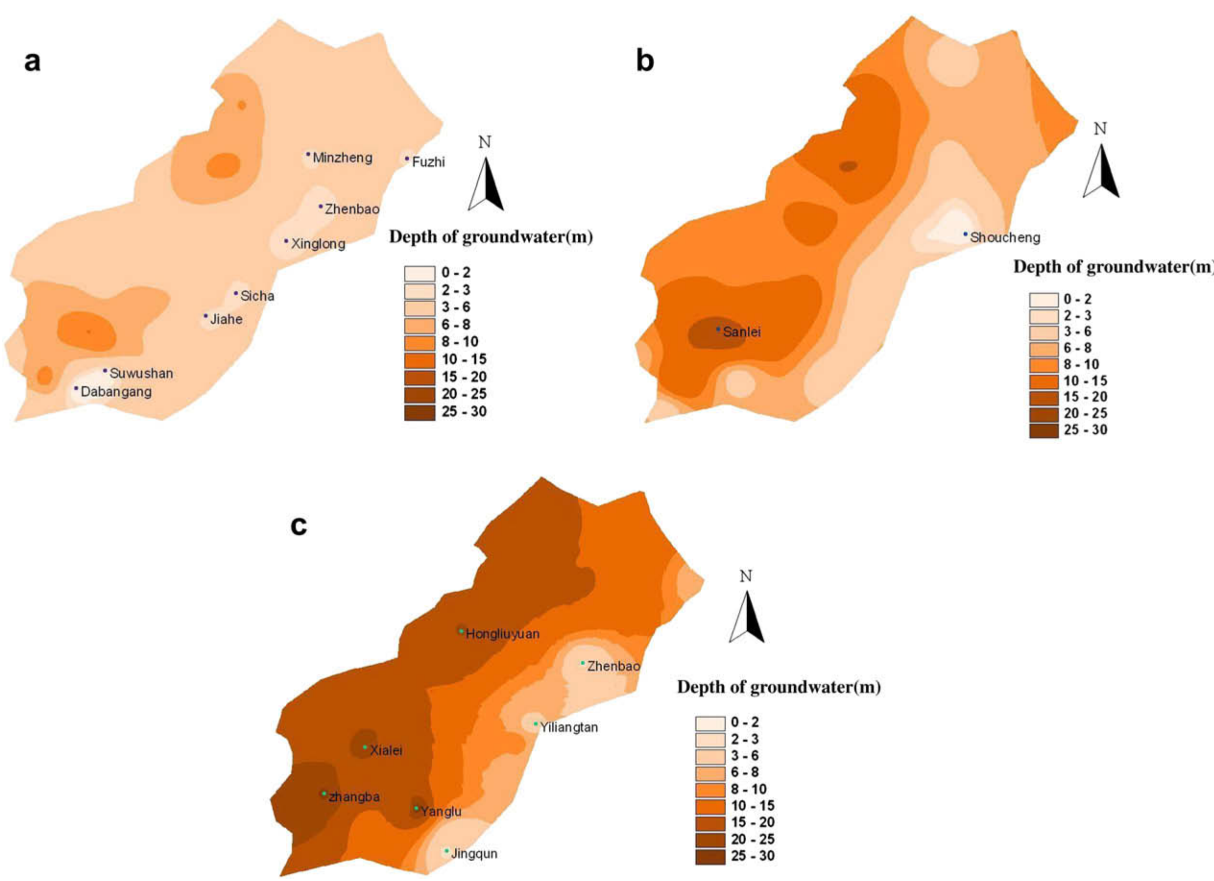

Fig. 6. Spatial variation of depth to groundwater obtained by the simple kriging method for 1981 (a), 1990 (b), and 2002 (c).

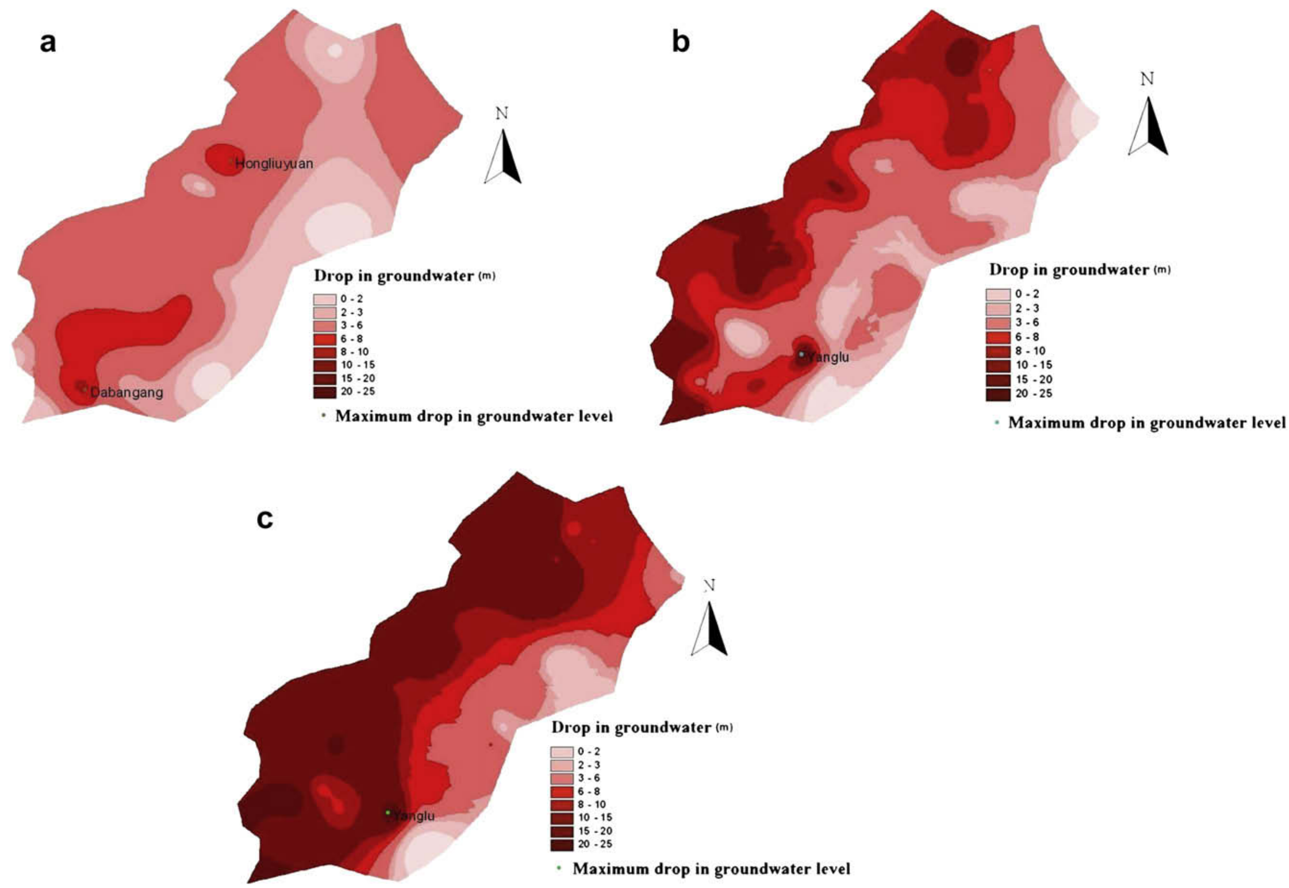

Fig. 7. Progressive drop in groundwater level in 1990 and 2002, using 1981 and 1990 as reference years (1981–1990(a), 1990–2002(b), 1981–2002(c)).

depths to groundwater in the region and land area with different depths to groundwater were obtained by GIS methods.

As shown in Table 2, although spatially the depth to groundwater in Minqin oasis varied greatly, the value of minimum, maximum, and average depth to groundwater in 1990 and 2002 were significantly greater than those in 1981. Over the past 22 years, the mean watertable decline has been about 10 m, an average decline of 0.47 m/yr. In the main, the depth to groundwater in the oasis was between 3–6 m in 1981, 6–10 m in 1990, and 10–20 m in 2002 (Fig. 4). Figs. 4 and 8 also indicate that the area with depth to groundwater below 6 m was 229,410 hm^2 in 1981, occupying 80% of the oasis; in 1990, the area with depth to groundwater below 6 m occupied only 21.5% of the oasis. However, in 2002, the area with depth to groundwater greater than 6 m was 268,410 hm^2, occupying 93.6% of the area.

In addition, the simulated depth to groundwater was obtained using Kendall's rank correlation test based on the depth to groundwater of eight selected observation wells in the past 22 years. Results showed that the depth to groundwater in the region declined significantly (Fig. 5 and Table 3).

In order to understand the distribution of groundwater resource in the future and provide a scientific basis for rational water allocation, autoregressive prediction equations of eight selected observation wells for depth to groundwater in the Minqin oasis were established based on the past 22 years of data.

$$H_t = a + bH_{t-1} + cH_{t-2} + dH_{t-3} + eH_{t-4} + fH_{t-5} \tag{16}$$

where H_t is the groundwater depth at year t; H_{t-1}, H_{t-2}, H_{t-3}, H_{t-4} and H_{t-5} are the depth to groundwater at year $t-1$, $t-2$, $t-3$, $t-4$, and $t-5$; and a, b, c, d, e, and f are parameters of the autoregressive model. Parameters of each autoregressive prediction equation for depth to groundwater of eight selected observation wells, and correlation coefficients between simulated values and measured values, are shown in Table 4. Here we see that correlation coefficients between the simulated and measured value in the past 17 years were greater than 0.9, indicating that the autoregressive model can quite accurately predict the depth to groundwater.

3.3. Spatial variation of depth to groundwater in Minqin oasis

We found that the depth to groundwater generally increased from the eastern end of the oasis to its western end (Fig. 6). The deepest groundwater was located in a zone in the southwestern part. In 1981, the area with depth to groundwater below 1 m was limited to about 350 hm^2 surrounding Dabangang in the western part of the oasis; other shallow areas, with depth to groundwater below 3 m, amounted to 18,500 hm^2 in areas surrounding Fuzhi, Minzheng, Xinglong, Zhenbao, Sicha, Jiahe, and Suwusan (Fig. 6a). In 1990, however, the area with depth to groundwater below 3 m had declined to 8750 hm^2 and only occurred near Shoucheng; in addition, an area of 5699 hm^2 with depth to groundwater of 15–20 m formed near Sanlei (Fig. 6b). By 2002, the area with depth to groundwater less than 2 m amounted to only 31 hm^2; the zone of 2–6 m depth had dwindled to 18,250 hm^2 and surrounded Jingqun, Zhenbao, and Yiliangtan (Fig. 6c). Moreover, the area with depth to groundwater greater than 20 m grew to 17,500 hm^2 in areas surrounding Hongliuyuan, Xialei, Yanglu, and Zhangba in the west (Fig. 6c).

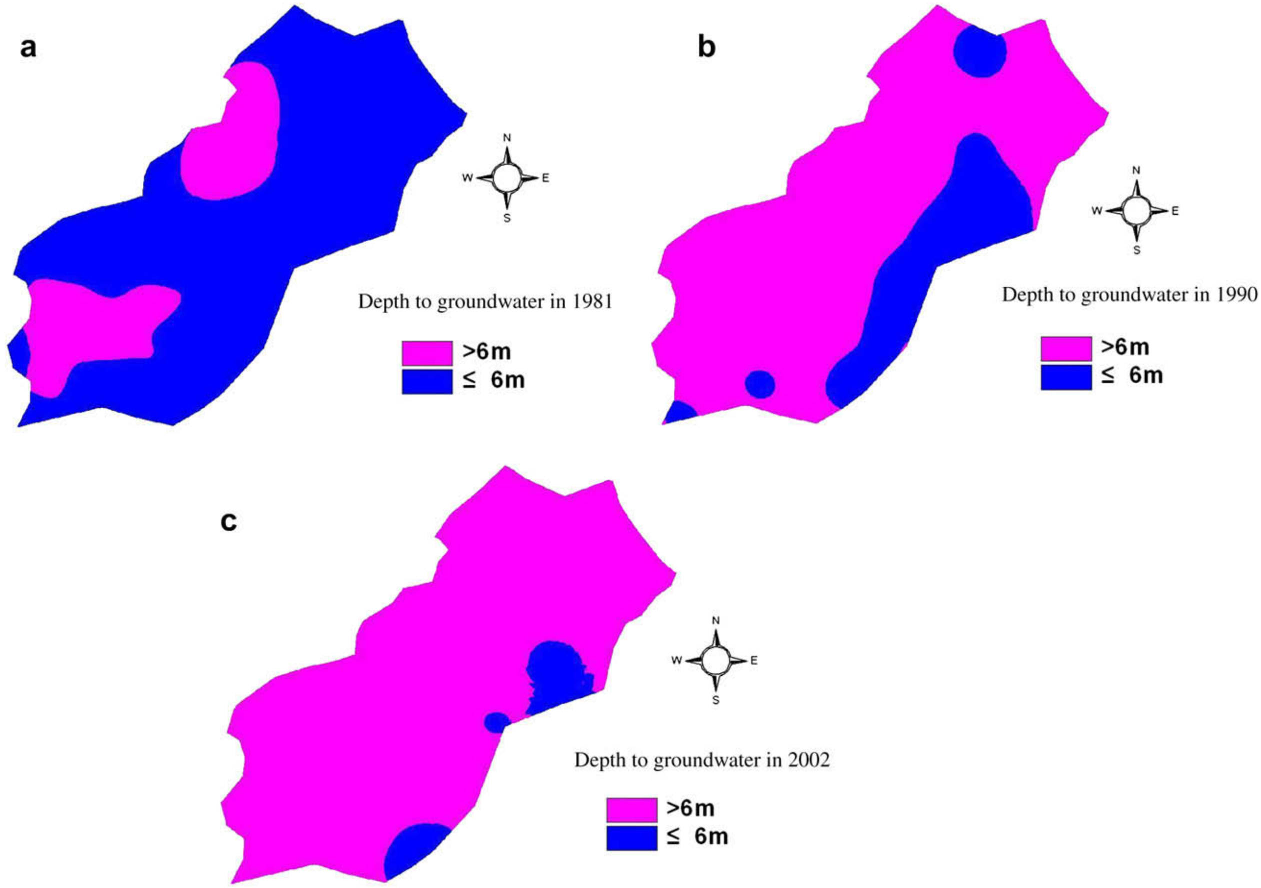

Fig. 8. Area distribution (>6 m and <6 m) obtained by the optimized spatial interpolation method.

Using 1981 and 1990 as reference years, we also plotted the progressive drop in groundwater level in 1990 and 2002, as shown in Fig. 7. During the period of 1981–1990, these plots show that two deep cones of depression (Fig. 7a) formed near Hongliuyuan (a depression of 6.8 m) and Dabangang (8.4 m). The greatest drops in groundwater levels occurred around Yanglu, where there was a drop of 17 m during the period of 1990–2002 (Fig. 7b), and near Zhangba, with a value of 27.6 m. Clearly, watertable levels have declined severely, especially in the mid-western part of the oasis where intense human activity has led to high exploitation of groundwater. In the past 22 years, the cone of depression in groundwater with maximum drop depth appeared near Yanglu, with the maximum drop in groundwater level of 22 m (Fig. 7c).

In the Minqin oasis, agricultural water use accounts for more than 95% of total water consumption. Because the region is limited in surface water resources, groundwater is the major source of irrigation water. Excessive groundwater extraction is the main cause of the severe decline in the water table. Improved irrigation channel efficiency, which leads to reduced groundwater recharge, has also contributed in a minor way to the decline. According to calculations of the Geological Research Institute of Gansu Province (Chang, 1994), annual total groundwater recharge was 229 million m^3 and the annual safe yield was 129 million m^3, but actual withdrawal was 445 million m^3. According to data from the Gansu Shiyang River Basin Administrative Bureau, irrigation channel efficiency increased from 0.30–0.35 in the 1950s to 0.54–0.72 in 2000. It is estimated that improved channel efficiency has reduced groundwater recharge by 9.9% in the irrigation region of Minqin oasis. Our results are in conformity with these data, showing that over the 22-year period the depth to groundwater was positively correlated ($R = 0.82$, $\alpha = 0.01$, confidence: 99%) with the volume of groundwater extraction and negatively correlated with inflow to Hongyashan Reservoir ($R = -0.65$, $\alpha = 0.05$, confidence: 95%).

4. Conclusions

We draw the following conclusions from this study:

(1) Simple kriging is the optimal method for interpolating depth to groundwater in this region (in terms of root mean squared errors and correlation coefficients between interpolated values and observed values). This conclusion is based on available data on the depth to groundwater in Minqin oasis over the past 22 years, which were in turn interpolated using kriging methods, inverse distance weighting (IDW), and the radial basis functions (RBF) method. Cross-validation was used to compare the various interpolation methods. Measures of uncertainty indicate that simple kriging had the lowest standard deviation of estimation errors (0.17) m and narrowest 95% prediction interval ($Z^* \pm 0.34$).

(2) The depth to groundwater in the oasis has increased greatly, with an average decline of 0.43 m per year. The deepest cone of depression occurs near Yanglu, where the lowest watertable depth was 22 m in 2002. The average depth to groundwater in the oasis was 3–6 m in 1981, 6–10 m in 1990, and 10–20 m in 2002. The percentage of the oasis with depth to groundwater of less than 6 m declined from 80% in 1981 to only 6.4% in 2002. The depth to groundwater in the mid-west of the oasis is greater than in its eastern parts. We attribute these declines largely to

excessive exploitation of groundwater, although increased irrigation channel efficiency has played a part.

(3) In the future we expect the cone of depression in groundwater in the oasis to increase even further unless drastic action is taken to curtail extraction rates.

Acknowledgements

We are grateful to research grants from the National Natural Science Foundation of China (40771034), the National High Technology Research and Development Program of China (863 Program, 2006AA100203), and PCSIRT (IRT0657).

References

Ashraf, M., Loftis, J.C., Hubbard, K.G., 1997. Application of geostatistics to evaluate partial weather station networks. Agricultural and Forest Meteorology 84, 255–271.
Caruso, C., Quarta, F., 1998. Interpolation methods comparison. Computers and Mathematics with Applications 35 (12), 109–126.
Chang, H.D., 1994. Water Conservancy Records of Minqin. Lanzhou University Press, Gansu.
Chen, S., Cowan, C.F., Grant, P.M., 1991. Orthogonal least squares learning algorithm for radial basis function networks. IEEE Transactions on Neural Networks 2, 302–309.
Collins, F.C., 1996. A comparison of spatial interpolation techniques in temperature estimation. In: Proceedings of the Third International Conference/Workshop on Integrating GIS and Environmental Modeling Santa Barbara, January 21–26.
Demuth, H., Beale, M., 1996. Neural Network Toolbox: User's Guide. The Math Works Inc., Natick, MA.
ESRI, 2004. Using Geostatistics Analyst. ESRI Inc.
Fang, S.M., Qian, Z.T., Li, Y.P., 2005. Comparison of four precipitation spatial interpolation methods in Gansu. Journal of Arid Land Resources and Environment 19 (3), 47–50.
Feng, J.M., Zhao, T.B., Hang, Y.J., 2004. Intercomparison of spatial interpolation based on observed precipitation data. Climatic and Environmental Research 9 (2), 261–277.
Hutchinson, M.F., 1995. Interpolating mean rainfall using thin plate smoothing splines. International Journal of Geographical Information Systems 9, 385–403.
Kang, S.Z., Su, X.L., Tong, L., Shi, P.Z., Yang, X.Y., Abe, Y., Du, T.S., Shen, Q.L., Zhang, J.H., 2004. The impacts of water-related human activities on the water–land environment of Shiyang river basin, an arid region in Northwest China. Hydrological Sciences Journal 49 (3), 413–427.
Kendall, M.G., Stuart, A., 1973. The Advanced Theory of Statistics. Griffin, London.
Kenneth, K.E., 1996. Conceptualization and characterization of groundwater systems using geographic information systems. Engineering Geology 42 (2–3), 111–118.
Kottegoda, N.T., 1980. Stochastic Water Resources Technology. Macmillan, London.
Li, J., You, S.C., Huang, J.F., 2006. Spatial interpolation method and spatial distribution characteristics of monthly mean temperature in China during 1961–2000. Ecology and Environment 15 (1), 109–114.
Li, X., Cheng, G.D., Lu, L., 2000. Comparison of spatial interpolation methods. Advances in Earth Sciences 15 (3), 260–265.
Li, X.Y., Song, D.M., Xiao, D.N., 2005. The variability of groundwater mineralization in Minqin oasis. Acta Geographica Sinica 60 (2), 319–327.
Theodossiou, N., Latinopoulos, P., 2006. Evaluation and optimisation of groundwater observation networks using the Kriging methodology. Environmental Modelling and Software 21 (7), 991–1000.
Theodossiou, N., Latinopoulos, P., 2007. Evaluation and optimisation of groundwater observation networks using the Kriging methodology. Environmental Modelling and Software 22 (3), 414.
Wang, J.L., Sun, J.S., Zhang, J.Y., 2004. Crop water requirement isoline based on GIS and geostatistics. Transactions of the CSAE 20 (5), 51–54.
Wei, J.H., Wang, G.Q., Li C.J., Shao, J.L., 2003. Recent advances associated with GIS in groundwater resources research (2), 94–98.
Xu, Y.Q., Cai, Y.L., 2005. GIS-based analysis on spatial-temporal change of groundwater level in the Hebei Plain. Acta Scientiarum Naturalium Universitatis Pekinensis 41 (2), 265–272.
Zhang, R.D., 2005. Theory and Application of Spatial Variation. Science Press, Beijing.
Zhang, Z.X., Kushwaha, R.L., 1999. Applications of neural networks to simulate soil–tool interaction and soil behavior. Canadian Agricultural Engineering 41, 119–125.